Supplementary information

Graphene film-functionalized germanium as chemically stable, electrically conductive, and biologically active substrate

Jinhua Li [a, 1], Gang Wang [b, e, 1], Wenjie Zhang [c, d, 1], Guodong Jin [a], Miao Zhang [b], Xinquan Jiang [c, d], Zengfeng Di [b, *], Xuanyong Liu [a, *], Xi Wang [b]

[a] *State Key Laboratory of High Performance Ceramics and Superfine Microstructure, Shanghai Institute of Ceramics, Chinese Academy of Sciences, Shanghai 200050, China.*

[b] *State Key Laboratory of Functional Materials for Informatics, Shanghai Institute of Microsystem and Information Technology, Chinese Academy of Sciences, Shanghai 200050,China.*

[c] *Department of Prosthodontics, College of Stomatology, Ninth People's Hospital, School of Medicine, Shanghai Jiao Tong University, Shanghai 200011, China.*

[d] *Oral Bioengineering Lab, Shanghai Research Institute of Stomatology, Ninth People's Hospital Affiliated to Shanghai Jiao Tong University, School of Medicine, Shanghai Key Laboratory of Stomatology, Shanghai 200011, China.*

[e] *School of Physical Science and Technology, Lanzhou University, Lanzhou 730000, China.*

* Corresponding Authors.

Prof. Xuanyong Liu

E-mail: xyliu@mail.sic.ac.cn

Prof. Zengfeng Di

E-mail: zfdi@mail.sim.ac.cn

[1] These authors contributed equally to this work.

Table S1. Related data for the energy level positions of germanium (Ge) and graphene.

Materials	Φ (eV)	E_g (eV)	χ (eV)	E_c (eV)	E_v (eV)
Ge		0.63[1]	4[2]	-4[α]	-4.63[α]
Graphene	4.23[3]				
Membrane protein		2.6-3.1[4, 5]			

Notes: E_0, vacuum level; E_F, Fermi level; Φ, work function; E_g, bandgap; χ, electron affinity; E_c, conduction band; E_v, valence band; α, calculated values.

Table S2. Cytological effects of graphene-based materials.

Graphene material	Preparation method	Transfer procedure	Highlights of the study	Ref.
FLG microsheets	Commercial product	Not involved (free state)	Graphene microsheets can enter cells through spontaneous membrane penetration at edge and corner sites and cause cytotoxicity.	[6]
Graphene and GO films	CVD and Hummers method	Transferred onto PDMS	Graphene film can better preconcentrate exogenetic osteogenic inducer and better promote osteogenic differentiation of MSCs than GO film.	[7]
Graphene film	CVD	Transferred onto TCPS	Graphene film can promote neurite sprouting and outgrowth of mouse hippocampal cells.	[8]
Graphene film	CVD	Transferred onto TCPS	Graphene film can enhance electrical signaling in neural networks of NSCs.	[9]
Graphene film	CVD	Transfer-free	Large-area monolayer graphene film can exhibit good biocompatibility and enhance osteogenic activity of MSCs.	α

Notes: FLG, few-layer graphene; PDMS, polydimethylsiloxane; TCPS, tissue culture polystyrene; MSCs, mesenchymal stem cells; NSCs, neural stem cells; α, the present work.

Table S3. Bacteriological effects of graphene-based materials.

Graphene material	Preparation method	Transfer procedure	Highlights of the study	Ref.
GO and rGO nanosheets	Hummers method	Not involved (free state)	Graphene nanosheets can destructively extract phospholipids from E. coli membranes and kill them.	[10]
GO and rGO papers	Hummers method and vacuum filtration	Not involved (freestanding)	GO and rGO papers can effectively inhibit growth of E. coli bacteria.	[11]
GO nanosheets modified cotton fabric	Hummers method and filtration	Transferred onto cotton fabric	GO-modified cotton fabrics can exhibit strong antibacterial property.	[12]
Graphene film	CVD	Transfer-free	Large-area monolayer graphene film can possess good antibacterial property.	α

Notes: α, the present work.

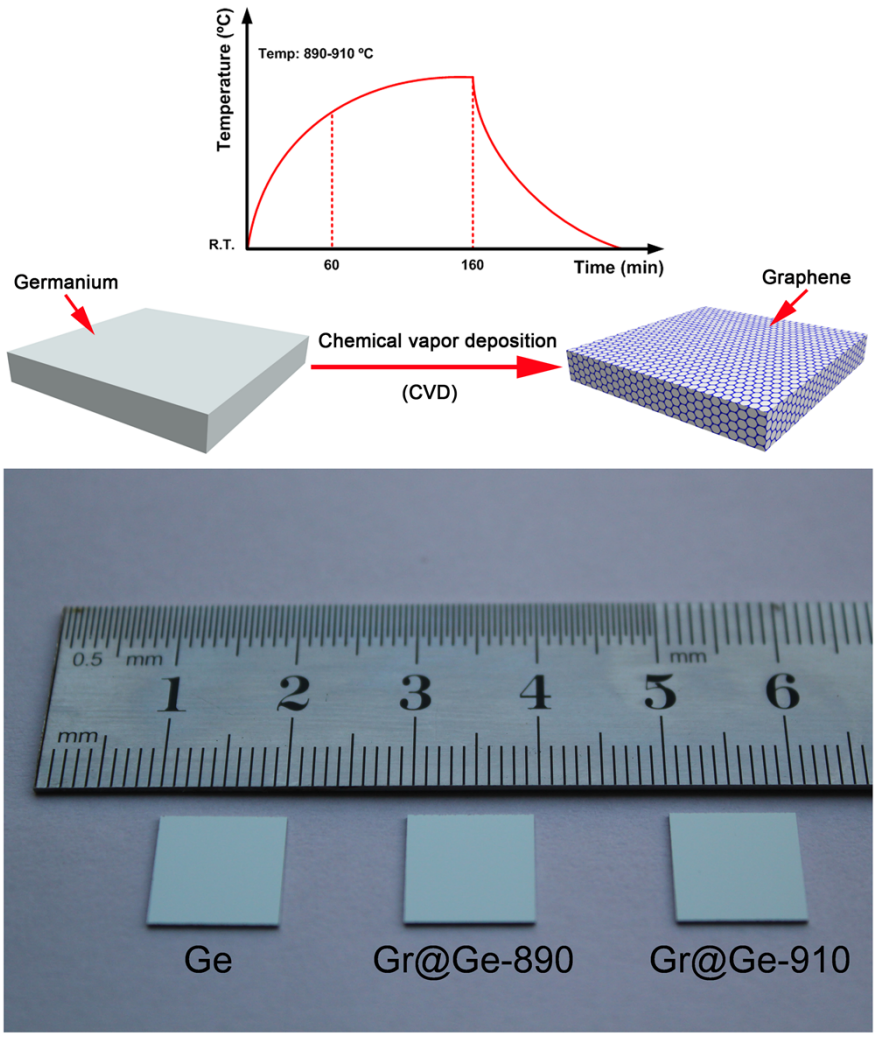

Supplementary Figure S1: (**Top panel**) Schematic illustration for the preparation of large-area monolayer graphene film on germanium substrate by chemical vapor deposition (CVD) method. (**Bottom panel**) Photographs of the pristine germanium (denoted as Ge), large-area graphene film grown on germanium at 890 °C (denoted as Gr@Ge-890) and 910 °C (denoted as Gr@Ge-910), respectively.

Figure S1 illustrates the schematic fabrication of monolayer graphene film on germanium substrate by CVD method (**top panel**), as well as the corresponding photographs of the pristine germanium and germanium substrate covered by large-area graphene films with different crystalline qualities, denoted as Ge, Gr@Ge-890 and Gr@Ge-910, respectively (**bottom panel**).

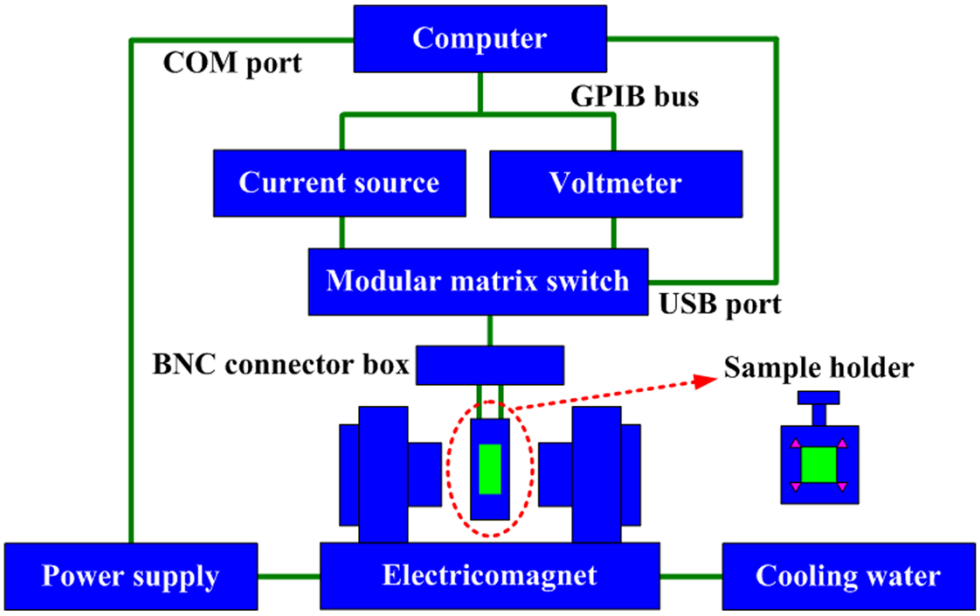

Supplementary Figure S2: Schematic illustration of the automatic four-probe Hall measurement setup with a Van der Pauw configuration.

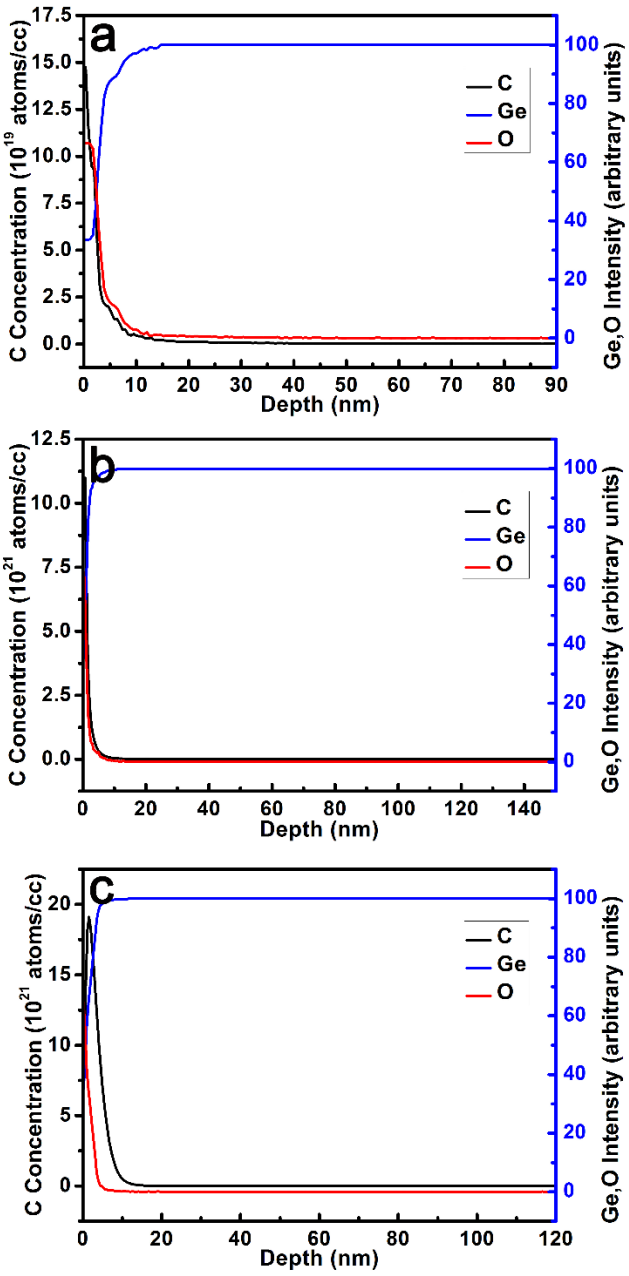

Supplementary Figure S3: (**a-c**) Secondary ion mass spectroscopy (SIMS) depth profiles indicating the carbon distribution in germanium substrate. (**a**), (**b**) and (**c**) correspond to Ge, Gr@Ge-890 and Gr@Ge-910, respectively.

Figure S3a-c further gives the SIMS analysis results from Ge, Gr@Ge-890 and Gr@Ge-910 specimens. **Figure S3a** shows the SIMS analysis for the pristine germanium substrate. The SIMS depth profiles in **Figure S3b** and **c** indicate the

limited carbon dissolution and diffusion in the germanium substrate after the growth of graphene film, which may account for the large-area growth of monolayered graphene film on germanium substrate, as an analogue of copper substrate.[13]

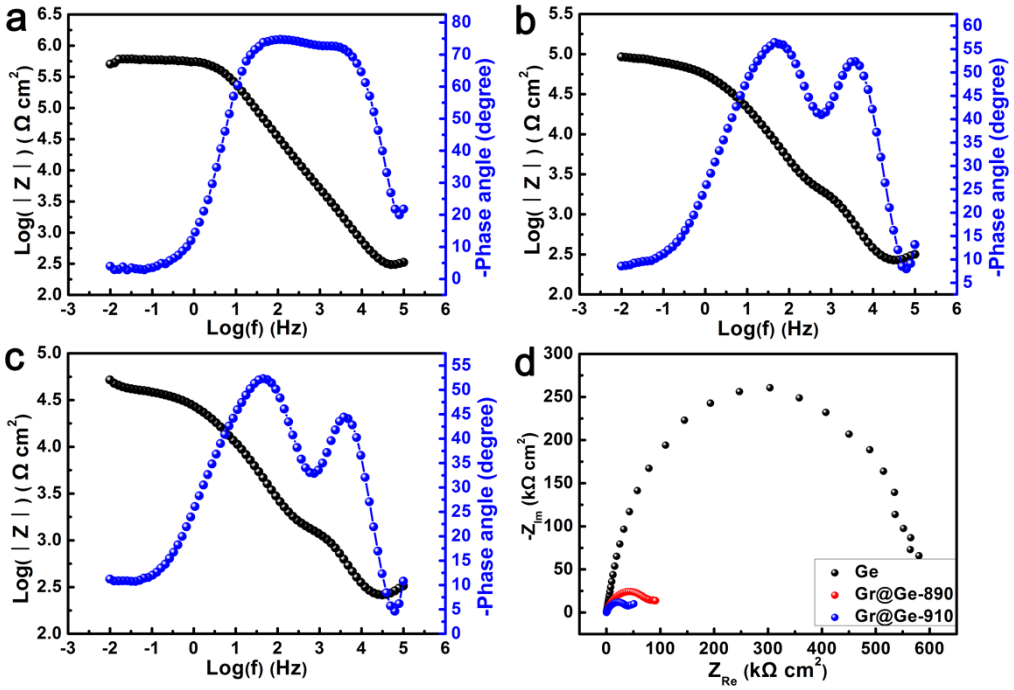

Supplementary Figure S4: Electrochemical impedance spectra of Ge, Gr@Ge-890 and Gr@Ge-910 in 0.9 wt% NaCl solution (**a-d**).

Electrochemical impedance spectra (EIS) were acquired at the open circuit potential, as shown in **Figure S4a-d**. The existence of graphene overlayer can reduce the corresponding impedance, especially for Gr@Ge-910. As shown in **Figure S4d**, with the graphene overlayer on Ge, the semicircle in Nyquist plot became shorter, indicating the decrease in solid state interface layer resistance and charge transfer resistance on the surface.[14]

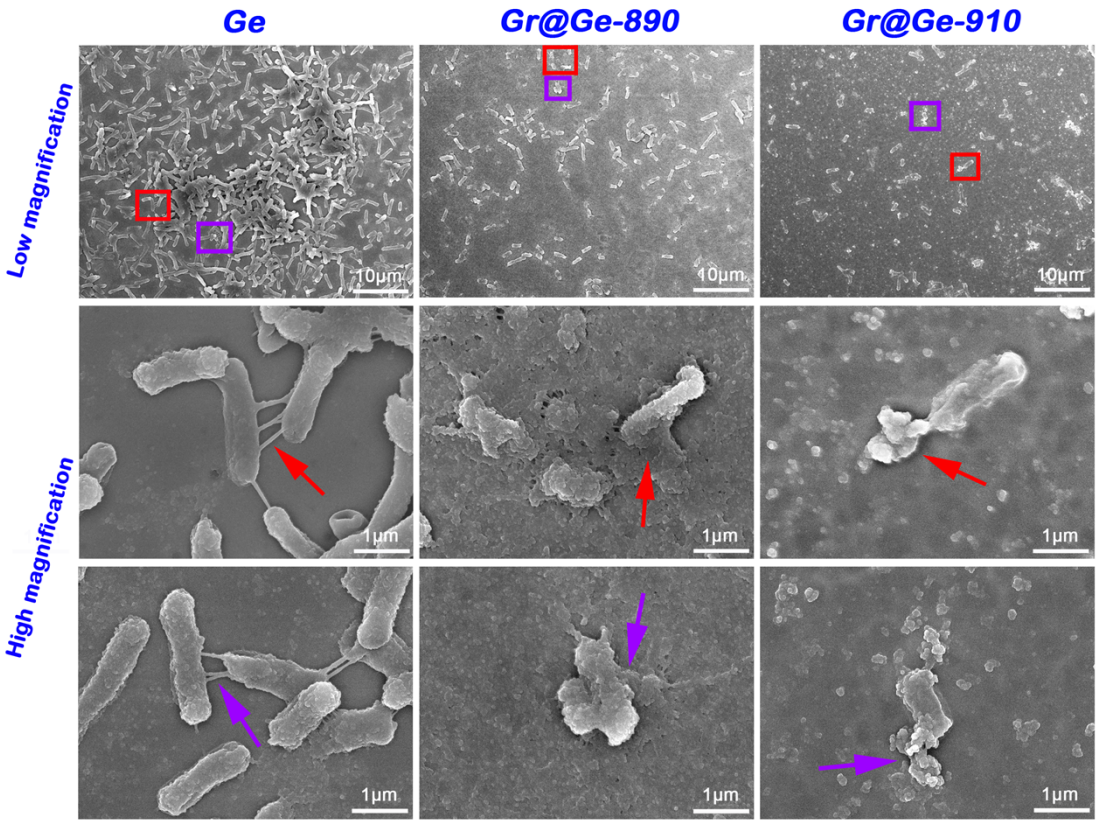

Supplementary Figure S5: Morphology of the E. coli bacteria that were seeded onto the samples at low and high magnifications examined by field-emission scanning electron microscopy (FESEM; Magellan 400, FEI, USA). The seeded concentration of bacteria is 10^7 CFU/mL. The red and violet arrows at high magnification correspond to the red and violet rectangular areas at low magnification, respectively.

Prior to the SEM examination, a droplet of bacterial solution with 10^7 CFU/mL was introduced onto the sample to a density of 60 μL/cm^2, incubated at 37 ºC for 24 h, fixed with 2.5 % glutaraldehyde solution, and dehydrated in gradient ethanol solutions (30, 50, 75, 90, 95, and 100 v/v%) for 10 min each sequentially, followed by drying in the hexamethyldisilizane (HMDS) and ethanol solution series and subsequent coating with platinum (Pt) for imaging via SEM.

In regard to the SEM results, the E. coli cells cultured on Ge surface were mostly

rod-shaped binary fission, which looked like no evident damage. Prevalent intercellular nanotubes can also be found on it (the red arrow at high magnification), bridging the neighboring bacteria and serving as a communication route, which indicated their exuberant vitality.[15] However, severe disruption of cytoplasmic membrane appeared on both the surfaces of Gr@Ge-890 and Gr@Ge-910, causing cytoplasma leakage and cell lysis, especially on the Gr@Ge-910.

Materials & Devices	Schematic diagram	Coating with germanium (Methods: PLD, ALD, etc.)	CVD growth of graphene
Ti & Ti alloys; Mg & Mg alloys; etc.	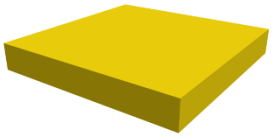	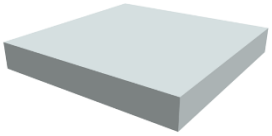	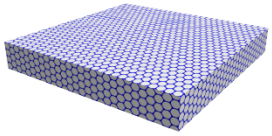
Artificial tooth; Bone screw; etc.			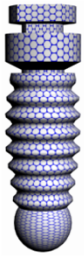

Supplementary Figure S6: Schematic illustration for the transfer-free graphene-based surface coating and modification of metallic biomaterials.

Nowadays, since the graphene has showed the promising potential to act as an osteogenic inducer and an antibiotic, it is quite an emergent need to develop its practical applications in biomedical fields, such as bone repair, tissue regeneration, stem cell therapy, etc.. In this work, we successfully fabricate the large-area graphene film on germanium surface. In contrast with previous reports on graphene films deposited by CVD on transition metals like copper and nickel, the used germanium substrate is relatively biocompatible since copper and nickel elements are commonly cytotoxic. One can naturally speculate that, if the germanium film is deposited onto a targeted substrate by an appropriate technique, then the high-quality graphene film will be grown on the germanium film by CVD method. Herein, we propose a rational design concept for the coating and modification of metallic biomaterials using transfer-free graphene film. In detail, two main steps are included: (i) A metallic substrate, such as titanium and titanium alloys, magnesium and magnesium alloys,

etc., is coated with a layer of germanium film by using an appropriate film coating technique, such as magnetron sputtering, pulsed laser deposition (PLD), atomic layer deposition (ALD), etc.; (ii) Subsequently, the high-quality and large-area monolayer graphene film is grown on the germanium film-coated metallic substrate by CVD method under the optimized parameters. The schematic illustration for the design concept is depicted in **Figure S6**. This rational design concept will open up the graphene-based surface coating and modification of metallic biomaterials and enlarge the graphene-based biomedical applications.

Notes and references

1. J. Li, G. Wang, H. Zhu, M. Zhang, X. Zheng, Z. Di, X. Liu and X. Wang, *Sci. Rep.*, 2014, **4**, 4359.
2. A. Dimoulas, P. Tsipas, A. Sotiropoulos and E. K. Evangelou, *Applied Physics Letters*, 2006, **89**, 252110-252113.
3. H. E. Romero, N. Shen, P. Joshi, H. R. Gutierrez, S. A. Tadigadapa, J. O. Sofo and P. C. Eklund, *ACS Nano*, 2008, **2**, 2037-2044.
4. D. D. Eley and D. I. Spivey, *Transactions of the Faraday Society*, 1960, **56**, 1432-1442.
5. T. A. Clarke, M. J. Edwards, A. J. Gates, A. Hall, G. F. White, J. Bradley, C. L. Reardon, L. Shi, A. S. Beliaev, M. J. Marshall, Z. Wang, N. J. Watmough, J. K. Fredrickson, J. M. Zachara, J. N. Butt and D. J. Richardson, *Proceedings of the National Academy of Sciences*, 2011, **108**, 9384-9389.
6. Y. Li, H. Yuan, A. von dem Bussche, M. Creighton, R. H. Hurt, A. B. Kane and H. Gao, *Proceedings of the National Academy of Sciences*, 2013, **110**, 12295-12300.
7. W. C. Lee, C. H. Y. X. Lim, H. Shi, L. A. L. Tang, Y. Wang, C. T. Lim and K. P. Loh, *ACS Nano*, 2011, **5**, 7334-7341.
8. N. Li, X. Zhang, Q. Song, R. Su, Q. Zhang, T. Kong, L. Liu, G. Jin, M. Tang and G. Cheng, *Biomaterials*, 2011, **32**, 9374-9382.
9. M. Tang, Q. Song, N. Li, Z. Jiang, R. Huang and G. Cheng, *Biomaterials*,

2013, **34**, 6402-6411.

10. Y. Tu, M. Lv, P. Xiu, T. Huynh, M. Zhang, M. Castelli, Z. Liu, Q. Huang, C. Fan, H. Fang and R. Zhou, *Nat Nano*, 2013, **8**, 594-601.

11. W. Hu, C. Peng, W. Luo, M. Lv, X. Li, D. Li, Q. Huang and C. Fan, *ACS Nano*, 2010, **4**, 4317-4323.

12. J. Zhao, B. Deng, M. Lv, J. Li, Y. Zhang, H. Jiang, C. Peng, J. Li, J. Shi, Q. Huang and C. Fan, *Advanced Healthcare Materials*, 2013, **2**, 1259-1266.

13. X. Li, W. Cai, J. An, S. Kim, J. Nah, D. Yang, R. Piner, A. Velamakanni, I. Jung, E. Tutuc, S. K. Banerjee, L. Colombo and R. S. Ruoff, *Science*, 2009, **324**, 1312-1314.

14. B.-L. He, B. Dong and H.-L. Li, *Electrochemistry Communications*, 2007, **9**, 425-430.

15. G. P. Dubey and S. Ben-Yehuda, *Cell*, 2011, **144**, 590-600.